IEEE Access
Multidisciplinary | Rapid Review | Open Access Journal

Received May 6, 2019, accepted June 25, 2019, date of publication July 5, 2019, date of current version August 19, 2019.

Digital Object Identifier 10.1109/ACCESS.2019.2927115

Variable Span Multistep Straightening Process for Long/Extra-Long Linear Guideways

YONGQUAN ZHANG[1,2], HONG LU[1], YONGJING WANG[2], XINBAO ZHANG[3], JINGLIN ZHANG[1], AND HE LING[1]

[1]School of Mechanical and Electronic Engineering, Wuhan University of Technology, Wuhan 430070, China
[2]Department of Mechanical Engineering, School of Engineering, University of Birmingham, Birmingham B15 2TT, U.K.
[3]School of Mechanical Science and Engineering, Huazhong University of Science and Technology, Wuhan 430074, China

Corresponding author: Xinbao Zhang (zhangxinbao1@hust.edu.cn)

This work was supported in part by the National Natural Science Foundation of China under Grant 51675393 and Grant 51505355, in part by the Special Fund for Key Project of Science and Technology of Hubei Province under Grant 2017AAA111, in part by the Fundamental Research Funds for the Central Universities under Grant 2016-YB-021, and in part by the Chinese Government Scholarship by the China Scholarship Council under Grant 201706950051.

ABSTRACT This paper presents a variable span multistep straightening process (VSMSP) to improve straightening accuracy and reduce the number of straightening steps for the multistep straightening of long linear guideways. It can also efficiently deal with the ineffectiveness caused by the single-step straightening process. The VSMSP adopts a sequence of three-point straightening processes with variable spans at different straightening positions. The paper presents the modeling of the behaviors of linear guideways in a straightening step and explains the use of the model to calculate the variables of the VSMSP. Key variables including span size, straightening position and straightening moment and stoke are optimized. The VSMSP and the model are validated experimentally on a straightening machine.

INDEX TERMS Pressure straightening, straightening strategy, variable span multistep straightening process, span-size searching algorithm, linear guideway.

I. INTRODUCTION

Linear guideways enable precise linear motion of machines and they have been widely adopted in many applications requiring high speed, heavy load and accurate positioning such as machine tools [1], [2]. Straightening of linear guideways is critical and can be challenging. The multi-roller straightening method is a possible approach but it generates complex residual stresses [3]–[6]. Compared with roller straightening methods, three-point straightening is more accurate and flexible, especially for the linear guideways with complex sectional features. It is now a popular method used in both rough and precise straightening [7], [8].

The process of three-point straightening has been widely studied. Kosel *et al.* [9] proposed an analytical model to predict springback after cyclic loading history, using the linear-hardening rheological material model and the large displacement theory. Zang *et al.* [10] used the three-point bending springback test to measure the Bauschinger effect, transient behavior and the permanent softening of metallic sheet in reverse loading. Ma *et al.* [11] investigated the effects of the offset of a neutral layer on the bending moment and the straightening springback, and how they are related to material properties, bar specifications, and straightening forces. Hou *et al.* [12] revealed the influence of punch radius on the elastic modulus, contact length and peak load of 6061 aluminum alloy. Mujika *et al.* [13] proposed the load-displacement models of the three-point and four-point straightening processes considering the variation of contact points between the workpiece and supports. Sofuoğlu *et al.* [14] investigated the springback behavior of the AA6082T6 tubes, including the springback level and acceleration in a three-point bending operation, considering indenter travel distance and wall thickness. Zhang *et al.* [15] considered neutral axis deviation caused by asymmetrical factors in linear guideways with complex sectional features and improved the prediction accuracy of three-point pressure straightening model. Song [16] established the load-deflection model, as well as the straightening stroke-deflection model, for the three-point straightening process of T-section rail under lateral loads, using the elastic-plastic power-law hardening material model.

The associate editor coordinating the review of this manuscript and approving it for publication was Zhixiong Peter Li.

However, the use of the single-step straightening process is limited by the design parameters of straightening facilities, including the range of supporting distance, the maximum straightening forces and straightening stroke. In addition, if a workpiece is in single-arc shape, the simulation and experimental results indicate that the unexpected deformation may occur if improper straightening parameters are used in a single-step straightening process, as shown in Fig. 1 [17]. Such an unexpected deformation is mainly caused by the large initial deflection and the long supporting distance.

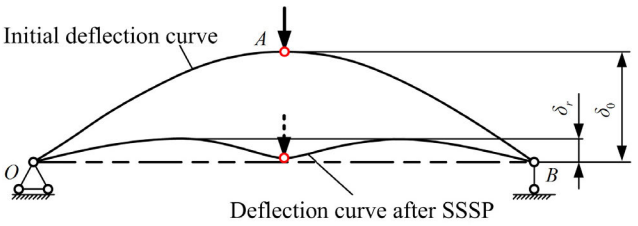

FIGURE 1. Schematic for the unexpected deformation during single-step straightening process (SSSP).

In order to minimize the straightening error of workpieces, multi-step straightening technology has been studied by many researchers. Kim and Chuang [18] developed a multi-step straightening system to minimize straightening errors of deflected shafts based on the load-deflection model of beams. By using the real-time deflection measurement devices, this system can identify straightening and material parameters online. The deflection pattern analysis and fuzzy self-learning method were employed to select straightening parameters in the multi-step process. Wang *et al.* [19] applied the multi-step method to the straightening of elevator guide rails using the load-deflection pressure straightening model. However, the angle of rotation at the supporting points generated by the straightening process was not discussed in this research, which was a sensitive parameter for the distribution of deflection during the multistep straightening process. Zhao and Song [17] also proposed a multi-step control strategy to determine the parameters of the straightening processes for long LSAW pipes, such as loading positions and straightening moments. Such a method can avoid the unexpected deformation that may be seen in a single-step straightening process, but this method can only be applied to the workpiece with a single-arc deflection curve.

Regarding long linear guideways 1000mm to 2500mm, or the extra-long ones exceeding 2500mm, up to 4000mm, the deflection curves may be more complex (e.g. in a 'S' shape or a multi-peak shape). Our previous work investigates the initial deflection-straightening stroke model and the angle of rotation of the deflection curve on the supporting points [20]. Then, a fixed-step multistep straightening process (FSMSP) was proposed for the long linear guideways with complex deflection curves, considering the angle of rotation caused by single-step straightening and the relationship between different straightening steps. However, the excessive straightening steps may induce a non-uniform distribution of residual stresses. It is also possible that more steps in a straightening process may cause more complex deflection curve.

The objective of this paper is to develop a variable span multistep straightening method, VSMSP, to further reduce the number of straightening steps and improve the straightening accuracy without introducing complex curves. Span-size searching algorithm is proposed to optimize the key variables in the VSMSP including span size, straightening position and straightening moment and stoke, thereby realizing the maximum performance of straightening facilities. The VSMSP for the long linear guideways is validated experimentally on a straightening machine.

II. MULTISTEP STRAIGHTENING PROCESS

A. THE INEFFECTIVENESS OF THE SINGLE-STEP STRAIGHTENING PROCESS

The single-step straightening process is limited by the capability of straightening facilities, including the range of supporting distance, the maximum straightening forces and straightening stroke. In addition, a failed straightening can be caused by long span size, or large initial deflection and straightening stroke. They may lead to an unexpected deformation, which changes the shape of the linear guideway from a single-arc shape to a more complex shape, as shown in Fig. 2. Failed straightening processes were investigated using a finite element method using the software ABAQUS.

Steel S55C, the most common material for making linear guideways, was used in the simulation. As demonstrated in Fig. 2, the linear guideway was on two supports. Its initial deflection was δ_0, and the load was at the middle of the supports on the opposite side. The 3D stress and reduced integration (C3D8R) were employed for all parts. The contact areas between the supports, load and workpiece were set up as hard contacts in the normal direction. A displacement was then applied simulating a straightening step. The deflection curve of linear guideway was measured using the path generated by the selected nodes on the guideways, before and after a straightening step.

The minimum and maximum span sizes were 200mm and 500mm with respect to the LG series linear guideways (Specification: 19 × 20mm). Such guideways can be used in making grinding, milling and drilling machines. The unexpected deformation is assumed to be avoided when $\delta_r \leq \delta_e$ (δ_r is the straightness error after a straightening step and δ_e is the required straightness error). Equation (1) describes the relationship between the supporting distance L_k and the corresponding maximum initial deflection δ_k with step size 20mm, as demonstrated in Fig. 3.

$$f : A \rightarrow B, L_m \in A,\ \delta_m \in \mathrm{B} \tag{1}$$

B. MULTISTEP STRAIGHTENING STRATEGY

The VSMSP can be demonstrated using the straightening machine ROSE-JZ50, and its operating setup is shown

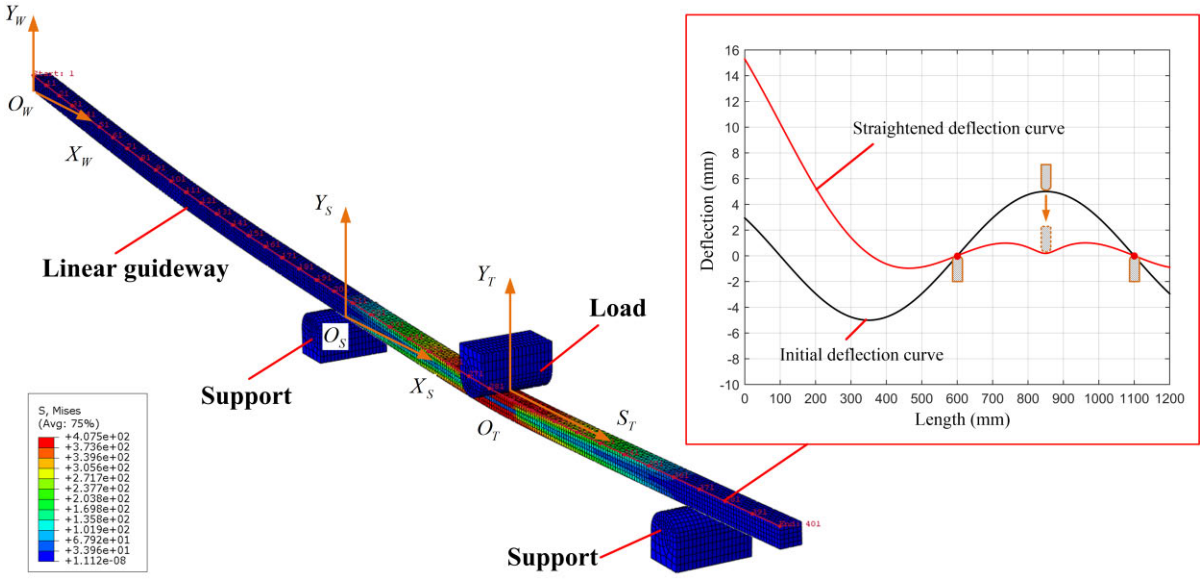

FIGURE 2. Deformed configuration in the simulation of single-step straightening process.

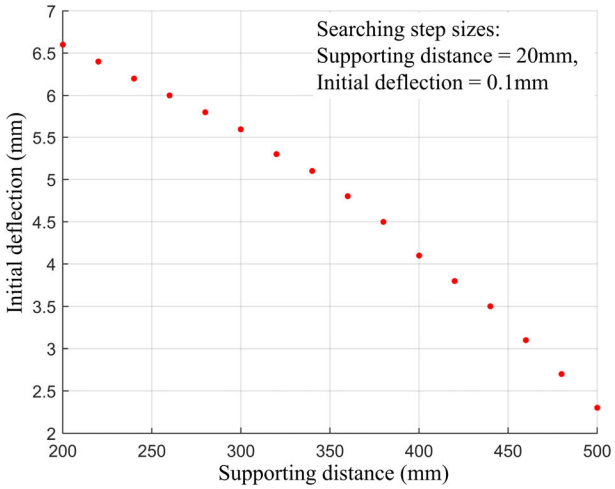

FIGURE 3. Deflection-distance distribution avoiding the unexpected deformation.

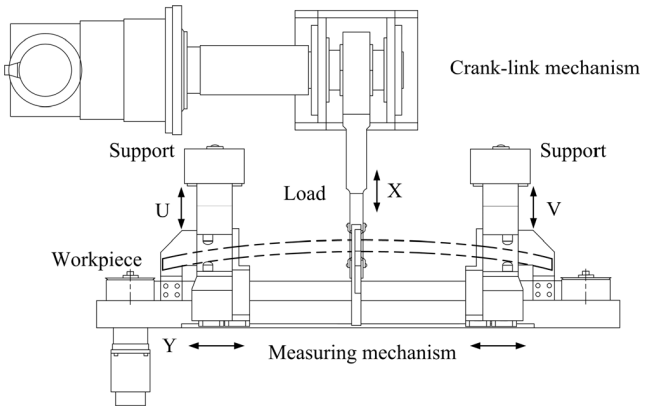

FIGURE 4. Straightening machine.

in Fig. 4. The linear guideway is divided into several segments that would be straightened separately using the three-point bending method. The straightening machine allows 4 types of movements in terms of straightening load (X axis) and supports (U, V and Y axes) as in Fig. 4. The straightening load, driven by a servo motor and a crank-link mechanism, can generate straightening forces in both tension and compression. It is horizontally installed on the machine foundation. The linear guideway can be clamped at the two supports. The movement of the two supports in combination with the clamping actions enables the feeding of linear guideway, as shown in Fig. 5. Furthermore, the supports offer reference surfaces for straightening in both tension and compression. Displacement sensors are fixed at the middle of the supports to detect the deflection of workpiece with an accuracy of 1μm.

The multi-step straightening strategy is illustrated as in Fig. 5, in which red lines represent the contact areas between the supports and workpiece. Initially, the workpiece is fed into the supports (V axis) by the roller conveyer as shown in Step 1 in Fig. 5. Then, the workpiece is clamped by supports (V axis) and fed to the position of Step 3. The workpiece can be fed by repeated motions of the V-axis supports as shown from Step 4 to 6. When the workpiece is in the area of U-axis supports, they take over the feeding task of workpiece (Step 7 to 9). The straightening process is carried out when the workpiece is at a planned position.

III. MATHEMATICAL MODEL FOR THE VSMSP

VSMSP consists of two stages: the major and fine stages. All segments are straightened in the major stage, but the shape

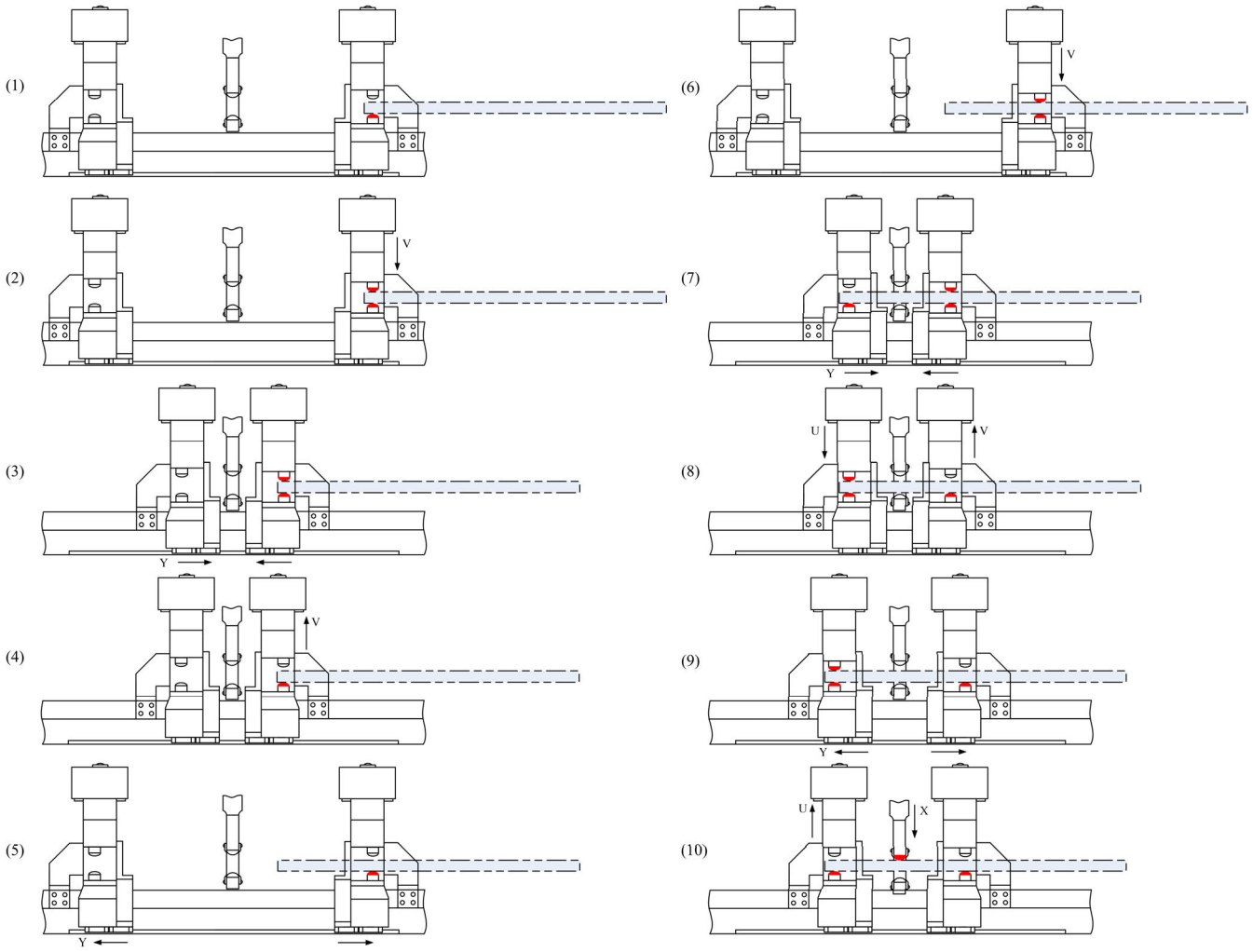

FIGURE 5. Multistep straightening strategy.

of the guideway may become a polyline. The aim of the fine stage is to correct from a polyline. There are a finite number of straightening steps based on the three-point straightening theory. VSMSP is mathematically modelled based on the span-size searching algorithm and the coordinate transformation of deflection curve.

A. COORDINATE SYSTEM DEFINITIONS

The deformation of the linear guideway can be two-dimensional and of three common types: single-arc shape, 'S' shape and multi-peak shape, as shown in Fig. 6.

Four types of coordinate systems are defined as shown in Fig. 7.

(1) $\{S_W : O_W - X_W Y_W\}$ and $\{S'_W : O'_W - X'_W Y'_W\}$ are ***the reference coordinate systems*** associated with the workpiece in tension and compression, and they represent the location of a workpiece in a straightening process.

(2) $\{S_M : O_M - X_M Y_M\}$ and $\{S'_M : O'_M - X'_M Y'_M\}$ are ***the measurement coordinate systems*** fixed on the workpiece in tension and compression, respectively. Initially, the originals of the measurement coordinate system and workpiece coordinate system are considered as the same.

(3) $\{S_S : O_S - X_S Y_S\}$ and $\{S'_S : O'_S - X'_S Y'_S\}$ are ***the straightening coordinate systems*** fixed on the edge of

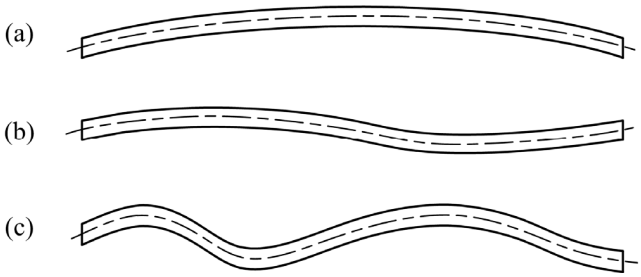

FIGURE 6. Types of deflection curves: (a) single-arc shape; (b) 'S' shape; (c) multi-peak shape.

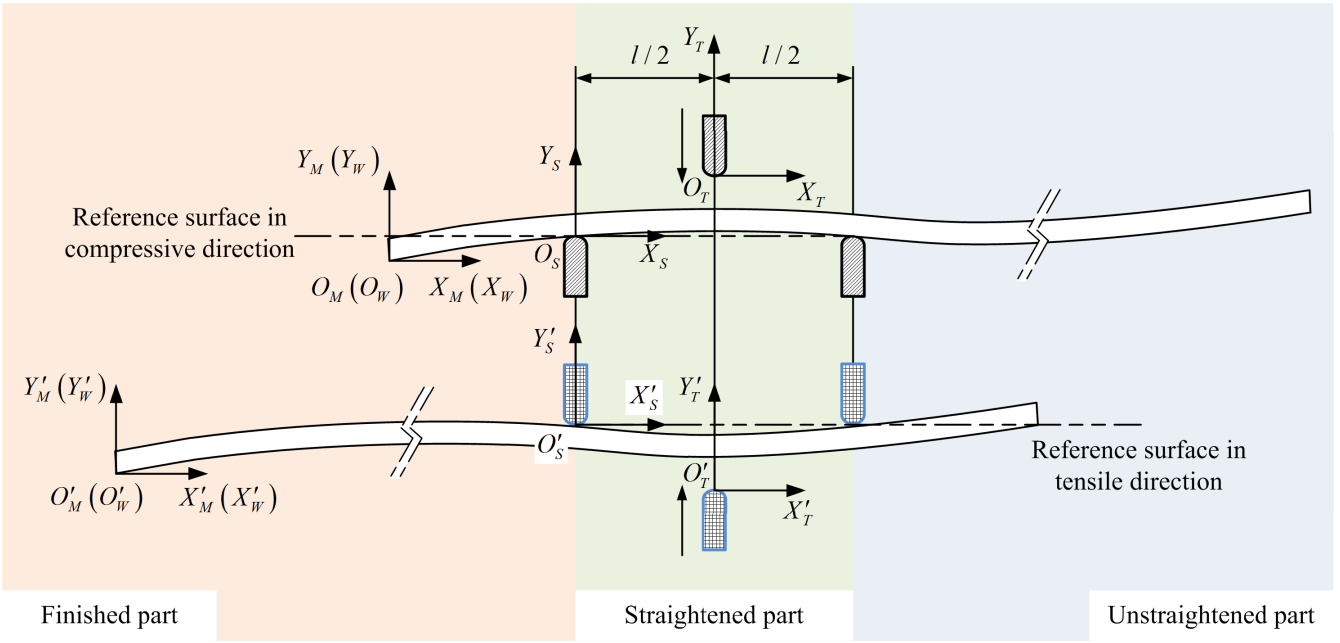

FIGURE 7. Definitions of coordinate systems.

supports in tension and compression. The deflection curves would be reconstructed after every straightening step.

(4) $\{S_T : O_T - X_T Y_T\}$ and $\{S'_T : O'_T - X'_T Y'_T\}$ represent ***the local coordinate systems*** on the load in tension and compression, and they are used to describe the straightening stroke.

The reference surfaces in tension and compression are on the edges of supports. In the mathematical model, the deflection curve is discretised into limited finite elements, defined as $\mathbf{a}_i^W = ({}^i x_j^W, {}^i y_j^W)$, where i represents the sequence number of straightening steps, and j is the sequence number of the elements on the deflection curve. During the single-step straightening process, the part of deflection curve inside two supporting points, defined as straightened part, would be corrected. The parts outside the supporting points, defined as finished and unstraightened parts, would rotate around the supporting points because of the angle of rotation generated by the bending process and springback. After every single-step straightening process, the deflection curve of a workpiece should be reconstructed by these three parts. They are represented as: finished part $\mathbf{a}_i^F = ({}^i x_j^F, {}^i y_j^F), j = 1, \ldots, {}^i n_F$, straightened part $\mathbf{a}_i^S = ({}^i x_j^S, {}^i y_j^S), j = {}^i n_F + 1, \ldots, {}^i n_S$, and unstraightened part $\mathbf{a}_i^U = ({}^i x_j^U, {}^i y_j^U), j = {}^i n_S + 1, \ldots, {}^i n_U$, in which ${}^i n_F$, ${}^i n_S$ and ${}^i n_U$ are varied with the straightening parameters of every step. When a straightening step is applied to a linear guideway, it is deformed to a polyline, and the turning points on the polyline are defined as control points, represented by $\mathbf{p}_{ij} = (x_{ij}, y_{ij})$.

B. MAJOR STRAIGHTENING STAGE

In the major stage, as shown in Fig. 8, the position of supports moves after each straightening step along the direction of the guideways. When a straightening step is finished, new control points are generated based on the current position of supports. The VSMSP mainly consists of feeding process, clamping process and straightening process, as shown in Fig. 5. Initially, the deflection curve is constructed as the discrete data based on the measured profile of linear guideway.

$$\mathbf{A}^M = \left[x_j^M, y_j^M, 1\right]^{\mathrm{T}}, \quad j \le \lceil L_W / L_r \rceil, \; j \in \mathrm{N}^* \tag{2}$$

where L_r is the defined resolution of the discrete deflection curve, and the element '1' is used for the calculation uniformity of the operation on the homogenous matrices.

As the origins of the workpiece coordinate system and the measurement coordinate system are the same, the deflection curve for the major straightening stage is initialized using the measured deflection curve.

$$\mathbf{A}_0^W = \mathbf{A}^M = \left[{}^0 x_j^M, {}^0 y_j^M, 1\right]^{\mathrm{T}} \tag{3}$$

In the following straightening steps, the start point of every step should be moved to the origin of a workpiece coordinate system, and the deflection curve needs to be reconstructed accordingly.

$$\mathbf{A}_i^W = \left[{}^i x_j^W, {}^i y_j^W, 1\right]^{\mathrm{T}}, \quad i \in \mathrm{N}^* \tag{4}$$

Span-size searching algorithm, the core step of VSMSP, is developed to determine the number of straightening steps. The optimization considers the dimensions of linear guideway, the capability of the straightening machine and the unexpected deformation.

The minimum and maximum span size are determined according to the dimensions of the linear guideway and the

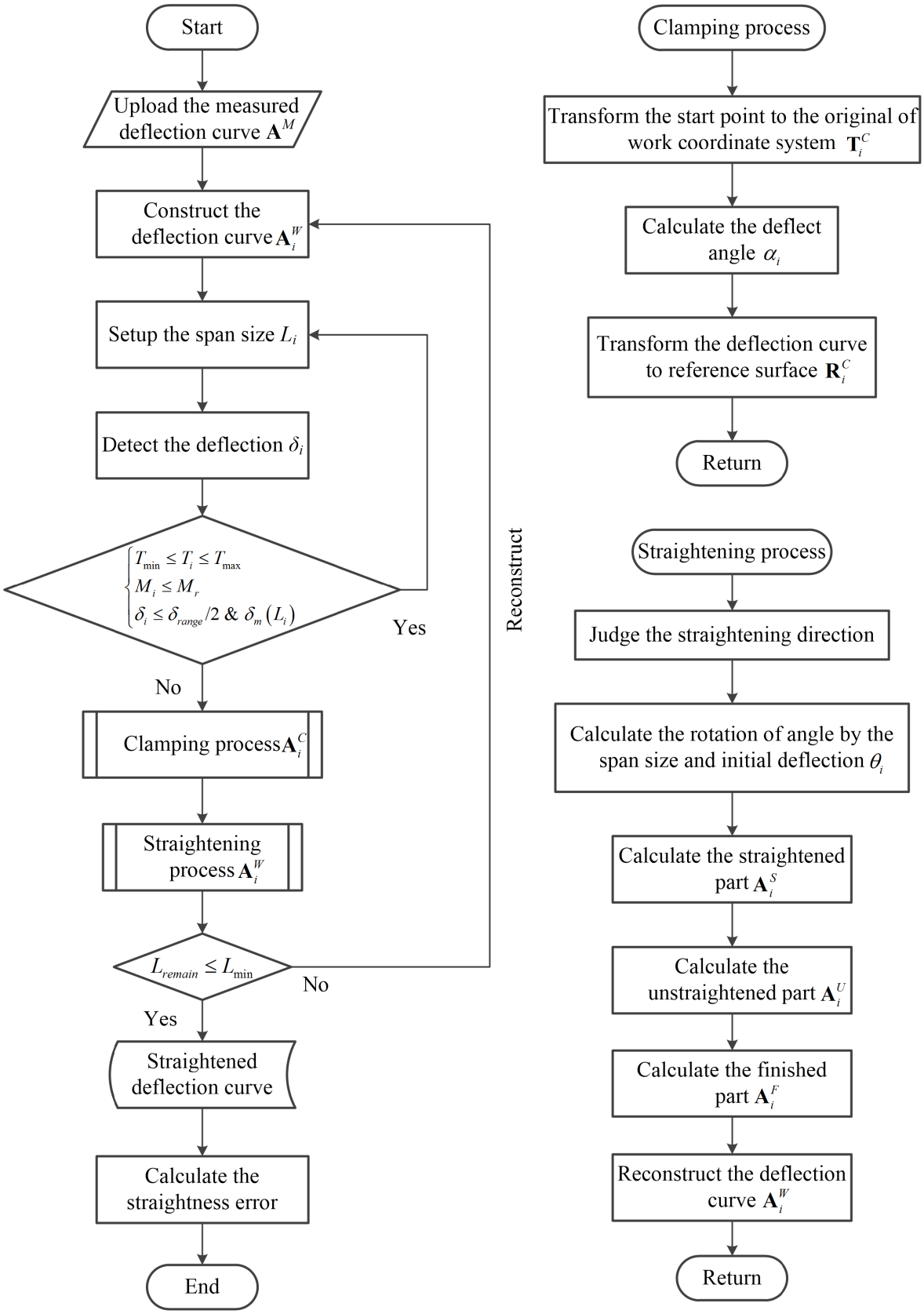

FIGURE 8. Flow chart for the mathematical model of the major straightening stage.

straightening machine determine. They can be given as

$$T_{\min} \le T_i \le T_{\max} \tag{5}$$

where, $T_{\min}$ and $T_{\max}$ are the minimum and maximum span size, respectively.

The nominal straightening moment is also determined by the payload of the straightening machine. In every straightening step, the straightening moment should be less than the rated straightening moment M_r.

$$M_i \le M_r \tag{6}$$

The straightening moment can be calculated as follows [20].

$$M_i = M_t \left(1.5 - 0.5\xi_i^2\right) \tag{7}$$

where, $M_t = BH^2\sigma_s/6$ is the elastic-limit moment; B and H are the width and height of the cross section respectively; σ_s is the yield stress.

The ξ_i is defined as the elastic-region ratio for different straightening steps.

$$\xi_i = H_{ti}/H \tag{8}$$

where, H_{ti} is the height of the elastic region in the straightening step i.

The measurement sensors are fixed at the middle of the supporting positions. As the linear guideway can be straightened in both tension and compression, the deflection of the linear guideway in single-step straightening process should be less than half of the measurement range.

$$\delta_i \le \delta_{range}/2 \tag{9}$$

To avoid unexpected deformation in the single-step straightening process, the corresponding deflection should be less than the standard deflection calculated by using (1).

$$\delta_i \le \delta_m\,(L_i) \tag{10}$$

L_{sz} is defined as the searching span size for the supporting distance. For every $L_i = L_m + kL_{sz}(k = 1, 2, 3\ldots)$, the straightening parameters of the single-step straightening step would be checked by using the constraint conditions, as concluded in (11). Additionally, if the remaining length of the linear guideway is less than the minimum span size for the straightening step, the deflection curve would be reconstructed in the next straightening stage.

$$\begin{cases} T_{\min} \le T_i \le T_{\max} \\ M_i \le M_r \\ \delta_i \le \delta_{range}/2 \& \delta_m\,(L_i) \end{cases} \tag{11}$$

Once the span size is determined, the deflection angle can be calculated, and the straightening parameters including straightening moment, straightening stroke, and the angle of rotation can be obtained using the analytical model of the single-step straightening process. In fact, the contact points between the linear guideway and the supports are the arbitrary positions on the edges of the supports. However, it has a minor influence on the accuracy of the analytical straightening model and the mathematical model of multistep straightening processes, and thus the contact points on the supports are assumed as the same during the whole straightening process.

Initially, the start point of a deflection curve in the current straightening step is moved to the origin of the workpiece coordinate system.

$$\begin{aligned} \mathbf{A}_i^O &= \begin{bmatrix} {}^ix_j^O \\ {}^iy_j^O \\ 1 \end{bmatrix} = \mathbf{T}_i^C \mathbf{A}_i^W \\ &= \begin{bmatrix} 1 & 0 & -L_i \\ 0 & 1 & 0 \\ 0 & 0 & 1 \end{bmatrix} \begin{bmatrix} {}^ix_j^W \\ {}^iy_j^W \\ 1 \end{bmatrix} \begin{pmatrix} a_{11} & a_{12} \\ a_{21} & a_{22} \end{pmatrix} \end{aligned} \tag{12}$$

Then, the deflect angle α_i can be calculated using the obtained span size L_i.

$$\alpha_i = \arctan\left({}^iy_k^W / {}^ix_k^W\right) \tag{13}$$

The deflection curve is rotated around the origin of workpiece coordinate system by α_i to describe the clamping process, as shown in Fig. 9.

$$\begin{aligned} \mathbf{A}_i^C &= \begin{bmatrix} {}^ix_j^C \\ {}^iy_j^C \\ 1 \end{bmatrix} = \mathbf{R}_i^C \mathbf{A}_i^O \\ &= \begin{bmatrix} \cos(\alpha_i) & -\sin(\alpha_i) & 0 \\ \sin(\alpha_i) & \cos(\alpha_i) & 0 \\ 0 & 0 & 1 \end{bmatrix} \begin{bmatrix} {}^ix_j^O \\ {}^iy_j^O \\ 1 \end{bmatrix} \end{aligned} \tag{14}$$

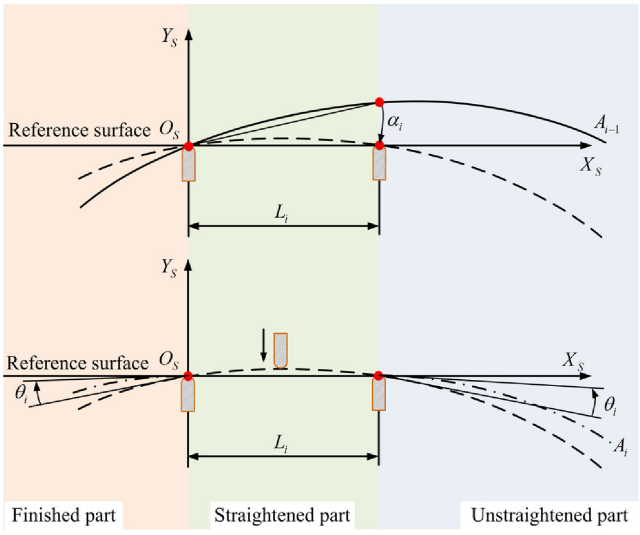

FIGURE 9. Schematic for the clamping and straightening processes.

The deflection curve after every straightening step is divided into three parts: finished, straightened and unstraightened parts. The straightened part is assumed to be straight after three-point straightening. Besides, due to the angle of rotation generated by the bending deformation during the

straightening, the finished and unstraightened parts would rotate around the start and end points of this straightening step, respectively. As a result, the bending direction of the deflection curve needs to be adjusted before the next straightening step.

If the deflection $\delta_i > 0$, the straightening step would generate in the tensile coordinate system $\{S_S : O_S - X_S Y_S\}$.The angle of rotation at the supporting points during single-step straightening process can be calculated as in [20].

$$\theta_i = \kappa_t l_t^{1/2}\left[(3l_t)^{1/2} - (3l_t - l)^{1/2}\right] - \theta_f + D \quad M_x > M_t \tag{15}$$

where, $\theta_f = M_x l/(4EI)$ is the angle of rotation during the elastic springback. M_x is the applied straightening moment. l is the distance between two fixed supports. E is Young's modulus of the material. I is the product of inertia for the rectangular cross section. κ_t is the elastic-limit curvature. $l_t = M_t l/(2M_x)$ is the length of the elastic deformation region. M_t is the elastic-limit moment. D is the coefficient to guarantee the continuity of the angle of rotation.

In terms of the single-step straightening process, the straightening stroke can be calculated by the springback of deflection and the initial deflection.

$$\delta_\Sigma = \delta_f + \delta_0 \tag{16}$$

where, $\delta_f = M_x l^2/(12EI)$ is the springback after unloading and δ_0 is the initial deflection of the linear guideway.

As shown in Fig. 9, the deflection curve in the finished part is obtained by the rotation of the curve $\mathbf{A}_i^W$ around the start point.

$$\begin{aligned}\mathbf{A}_i^F &= \begin{bmatrix} {}^i x_j^F \\ {}^i y_j^F \\ 1 \end{bmatrix} = \mathbf{R}_i^{RA}\mathbf{A}_i^W \\ &= \begin{bmatrix} \cos(\theta_i) & -\sin(\theta_i) & 0 \\ \sin(\theta_i) & \cos(\theta_i) & 0 \\ 0 & 0 & 1 \end{bmatrix}\begin{bmatrix} {}^i x_j^W \\ {}^i y_j^W \\ 1 \end{bmatrix}\end{aligned} \tag{17}$$

As the deflection curve of the straightened part is assumed to be straight, the y-axis value of the deflection curve always equals to zero.

$$\mathbf{A}_i^S = \left[{}^i x_j^W, 0, 1\right]^{\mathrm{T}} \tag{18}$$

The deflection curve $\mathbf{A}_i^W$ is rotated by θ_i around the end point of this straightening step, thereby calculating the deflection curve of the unstraightened part.

$$\begin{aligned}\mathbf{A}_i^U &= \begin{bmatrix} {}^i x_j^U \\ {}^i y_j^U \\ 1 \end{bmatrix} = \mathbf{R}_i^{RA}\mathbf{A}_i^W \\ &= \begin{bmatrix} \cos(\theta_i) & \sin(\theta_i) & 0 \\ -\sin(\theta_i) & \cos(\theta_i) & 0 \\ 0 & 0 & 1 \end{bmatrix}\begin{bmatrix} {}^i x_j^W \\ {}^i y_j^W \\ 1 \end{bmatrix}\end{aligned} \tag{19}$$

In sum, the deflection curve after this straightening step consists of the finished part, straightened part and unstraightened part.

$$\mathbf{a}_i^W = \begin{cases} \mathbf{a}_i^F = \left({}^i x_j^F, {}^i y_j^F\right) \\ \mathbf{a}_i^S = \left({}^i x_j^S, {}^i y_j^S\right) \\ \mathbf{a}_i^U = \left({}^i x_j^U, {}^i y_j^U\right) \end{cases} \tag{20}$$

If the deflection $\delta_i < 0$, the straightening process should be performed in the coordinate system $\left\{S_S' : O_S' - X_S' Y_S'\right\}$. To simplify the mathematical model, the width of the linear guideway is compensated to the straightening stroke in compression.

After the straightening step, the deflection curve can be reconstructed based on the finished, straightened and unstraightened parts, and the reconstructed curve would be used as the initial deflection curve in the next straightening step.

C. FINE STRAIGHTENING STAGE

In the major straightening stage, the deflection curve of linear guideway is reconstructed as a polyline. The points on this polyline are defined as the control points of the deflection curve.

$$\mathbf{p}_{ig} = \left(x_{ig}, y_{ig}\right) \quad i = 1, 2, \ldots, n \text{ and } g = 1, 2, \ldots, n+2 \tag{21}$$

where, i is the straightening step and g is the sequence number of control points.

The algorithm of the fine straightening stage is given in Fig. 10. After the major straightening stage, the deflection curve of linear guideway could be reconstructed to be a polyline. The angles on the control points, except the start and end points are then calculated, which are employed to recognize the profile characteristics of the deflection curve. The angles are sequenced by the magnitude in the following straightening steps. When a straightening sequence is determined, the straightening would be conducted step by step until the straightness of the deflection curve meets the requirements. The constraint function for the fine straightening stage can be expressed as

$$\begin{cases} \min \delta_r \\ s.t. \begin{cases} T_{\min} \le T_i \le T_{\max} \\ M_i \le M_r \\ \delta_i \le \delta_{range}/2 \\ \delta_i \le \delta_m(L_i) \end{cases} \\ x \in \left\{x_{ig}\right\} \end{cases} \tag{22}$$

In the fine straightening stage, the span size is to look for control points that would be regarded as the straightening positions. In addition to the constraints in the major straightening stage, the span size is also restricted by the distances between two adjacent control points. Finally, the straightness error of the deflection curve is evaluated using minimum zone straightness criterion defined by the ASME Y14.5.1M.

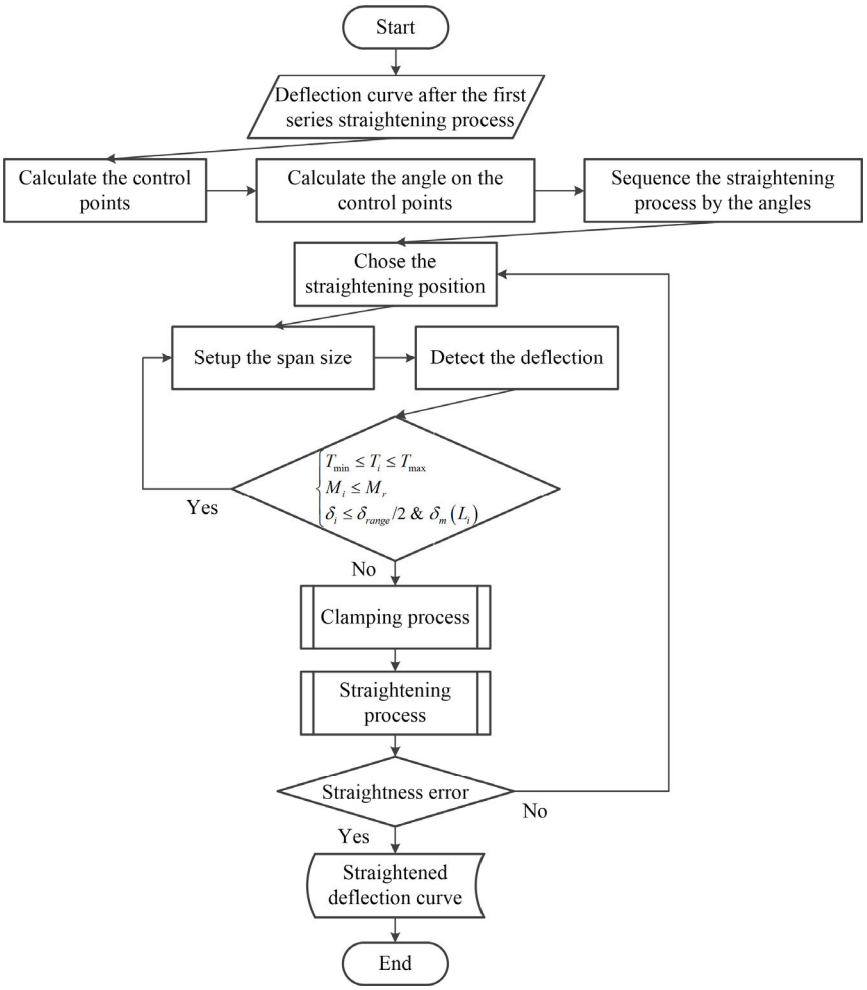

FIGURE 10. Flow chart for the fine straightening stage.

IV. ANALYSIS OF VSMSP

In terms of the three typical deflection curves (including single-arc shape, 'S' shape and multi-peak shape), the accuracy analysis of VSMSP was performed using the symbolic math toolbox of MATLAB. In each section, the profile of the deflection curve was reshaped after every straightening step. Additionally, the straightness errors after the major and fine straightening stages were compared in every straightening case. The following initial values of the parameters for the VSMSP of the workpiece with single arc shape are used: $B = 19$mm, $H = 20$mm, $\sigma_s = 415$Mpa, $\varepsilon_t = 0.3\%$, $E = 210$Gpa, the length of sample workpiece $L_W = 1000mm$.

The linear guideway is made of high-quality liquid steel, which is cast to the square billet based on the continuous casting technology. Then, the linear guideway billet with cross-section features is forged using the continuous steel rolling process. These processes are the main reasons causing the straightness error of the linear guideway billet. In addition, heat treatment process can also deform the linear guideway billet. The straightness error should be compensated by the milling and grinding processes. To increase efficiency and productivity, the milling and grinding allowances should be minimized. Taking the form error of cross section, surface roughness and production cost into account, the straightness error is normally required to be under 0.8 mm per meter in the rough straightening process.

A. SINGLE-ARC DEFLECTION CURVE

A curve simulating a single-arc deflection curve was created by using a sine function $f(x) = 5\sin(\pi x/L_W)$ over [0,1000] with a segment size of 1mm along the length, and the straightness error of which was 5mm. Based on constraint conditions, the major straightening stage consisted of 2 steps, and the straightening parameters were listed in Table 1. The deflection curves in the major straightening stage were demonstrated in Fig. 11. The bending direction was reversed after the major straightening stage, and the straightness error was calculated to be 5.967mm, which was even bigger than the initial deflection.

After the major straightening stage, the horizontal coordinates of control points on the deflection curve were 0, 500 and 1000mm. As there was only one angle on the straightened

TABLE 1. The parameters of the major straightening stage for single-arc deflection curve.

No.	1	2
Span size (mm)	500	500
Initial deflection (mm)	1.036	1.153
Standard deflection (mm)	2.300	2.300
Deflect angle (rad)	0.999e-2	0.192e-2
The angle of rotation (rad)	0.022	0.022
Straightening stroke (mm)	5.463	5.613
Straightening moment (Mpa)	4.847e5	4.883e5
Final straightness (mm)	5.967	

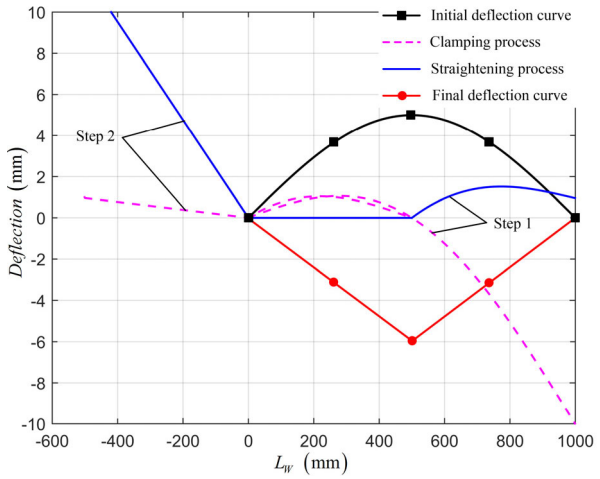

FIGURE 11. Theoretical results of the major straightening stage for the single-arc deflection curve.

TABLE 2. He parameters of the fine straightening stage for the single-arc deflection curve.

No.	3
The angle of the point (rad)	3.118
Straightening position (mm)	500
Span size (mm)	240
Initial deflection (mm)	1.417
Standard deflection (mm)	6.200
The angle of rotation (rad)	0.011
Straightening stroke (mm)	2.574
Straightening moment (Mpa)	5.500e5
Final straightness (mm)	0.545

deflection curve, it was then straightened on the second control point, as listed in Table 2. After the fine straightening stage as shown in Fig. 12, the straightness error was improved to 0.545mm.

As shown in Fig. 13, L, T, and n represent supporting distance, overlap distance and the quantity of straightening steps in the FSMSP, respectively. It can be noticed that the straightness error was 2.050mm when the 5-step FSMSP was applied in this case, which was less than that using 3-step

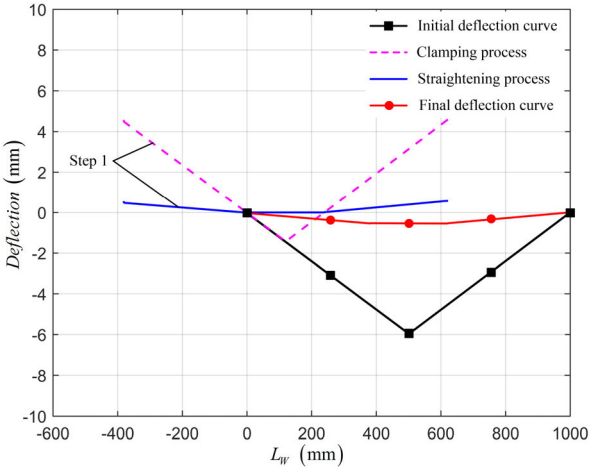

FIGURE 12. Theoretical results of the fine straightening stage for the single-arc deflection curve.

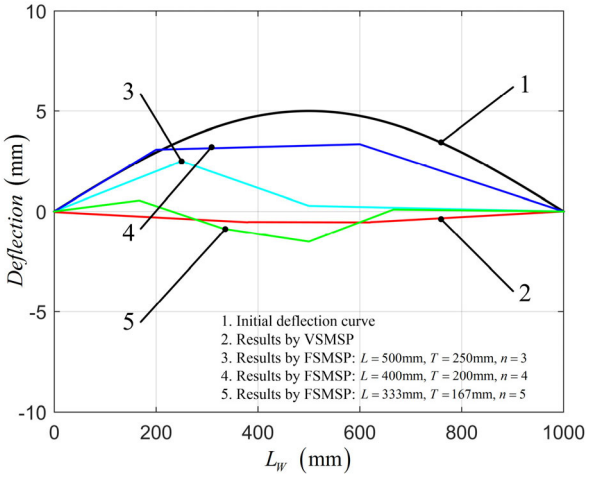

FIGURE 13. Comparison of theoretical results by VSMSP and FSVSP for the single-arc deflection curve.

and 4-step FSMSP. However, the straightness error can reach 0.545mm after 4-step VSMSP.

B. 'S'-SHAPE DEFLECTION CURVE

In the straightening case of 'S'-shape deflection curve, a curve simulating the deflection was created by using a sine function $f(x) = 5\sin(2\pi x/L_W)$ over [0,1000], and the segment size for the length was chosen to be 1mm. It can be noticed that the initial defection was 10mm. Calculated using the mathematical model of the VSMSP, the major straightening stage was divided into 2 steps, and the span sizes of which were 420mm and 440mm, respectively. The major straightening stage was then aborted as the residual length of the deflection curve was less than the minimum span size. The corresponding straightening parameters were listed in Table 3, and the deflection curves in the major straightening stage were demonstrated in Fig. 14. After the major straightening stage, the straightening error was calculated

TABLE 3. The parameters of the major straightening stage for 'S'-shape deflection curve.

No.	1	2
Span size (mm)	420	440
Initial deflection (mm)	3.651	3.114
Standard deflection (mm)	3.800	3.500
Deflect angle(rad)	0.581e-2	-0.180e-2
The angle of rotation (rad)	0.018	0.019
Straightening stroke (mm)	7.140	6.893
Straightening moment (Mpa)	5.439e5	5.343e5
Final straightness (mm)	3.786	

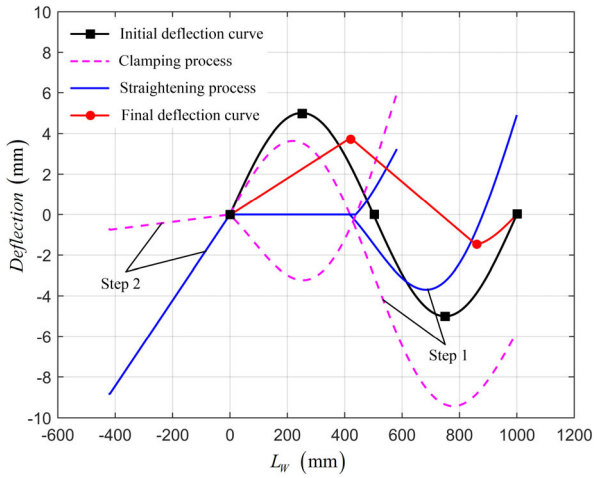

FIGURE 14. Theoretical results of the major straightening stage for the 'S'-shape deflection curve.

TABLE 4. The parameters of the fine straightening stage for the 'S'-shape deflection curve.

No.	3	4
The angle of the point (rad)	3.121	3.119
Straightening position (mm)	860	420
Span size (mm)	240	240
Initial deflection (mm)	1.256	1.319
Standard deflection (mm)	6.2	6.2
The angle of rotation (rad)	0.011	0.011
Straightening stroke (mm)	2.404	2.472
Straightening moment (Mpa)	5.456e5	5.474e5
Final straightness (mm)	2.743	0.181

to be 3.786mm, which did not meet the requirements of straightness, thereby requiring the fine straightening stage.

After the major straightening stage, the horizontal coordinates of control points on the deflection curve were 0, 420, 860 and 1000mm. The angles on the deflection curve were then evaluated and sorted by the influences on the deflection curve. As listed in Table 4, the first step in the fine straightening stage would be performed on the third control point, and the straightness was calculated as 2.743mm, which did not meet the straightness's requirements either. The second step in the fine straightening stage was then performed on

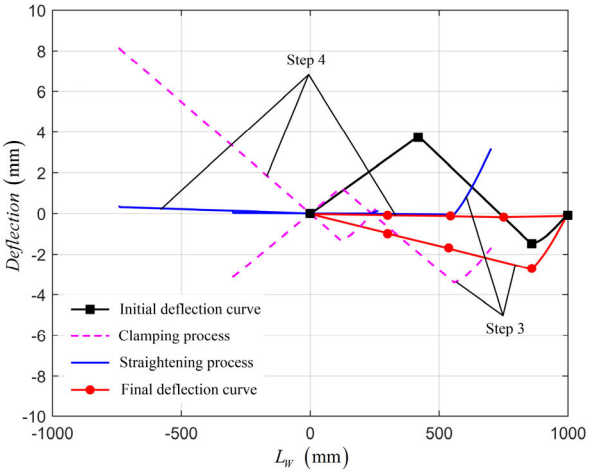

FIGURE 15. Theoretical results of the fine straightening stage for the 'S'-shape deflection curve.

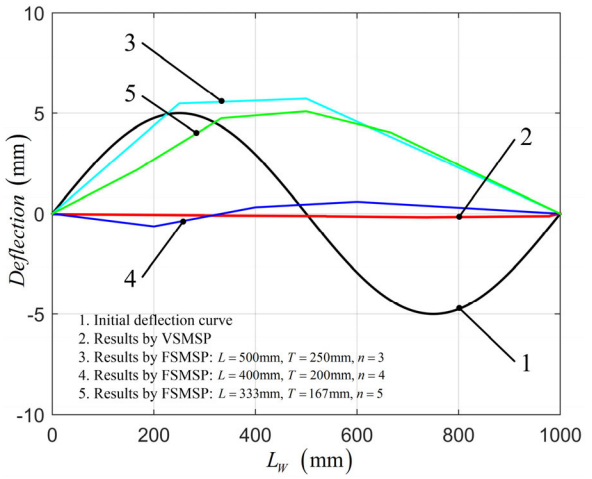

FIGURE 16. Comparison of theoretical results by VSMSP and FSVSP for the 'S'-shape deflection curve.

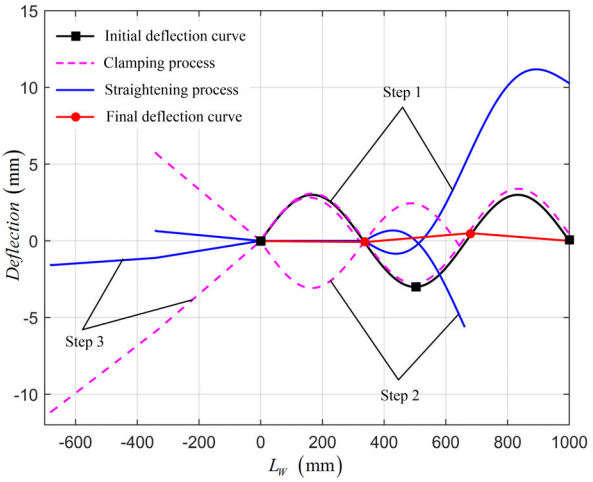

FIGURE 17. Theoretical results of the major straightening stage for the multi-peak deflection curve.

the second control point. It can be noticed that the straightness of the deflection curve has been significantly improved after the fine straightening stage as shown in Fig. 15. As shown

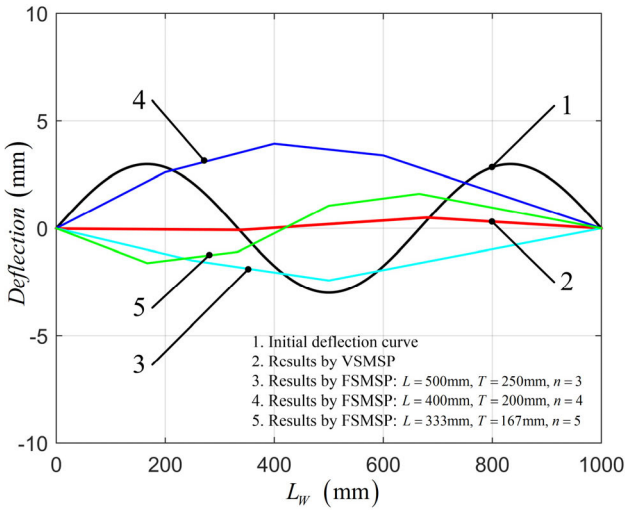

FIGURE 18. Comparison of theoretical results by VSMSP and FSVSP for the multi-peak deflection curve.

TABLE 5. The parameters of the major straightening stage for multi-peak deflection curve.

No.	1	2	3
Span size (mm)	340	340	320
Initial deflection (mm)	3.120	3.0831	2.866
Standard deflection (mm)	5.100	5.100	5.300
Deflect angle (rad)	-0.047e-2	1.679e-2	-1.734e-2
The angle of rotation (rad)	0.015	0.015	0.014
Straightening stroke (mm)	5.444	5.418	4.953
Straightening moment (Mpa)	5.534e5	5.528e5	5.543e5
Final straightness (mm)		0.577	

TABLE 6. The parameters of the major straightening stage for multi-peak deflection curve.

No.	1	2	3
Span size (mm)	320	320	340
Initial deflection (mm)	4.678	4.5946	5.022
Standard deflection (mm)	5.300	5.300	5.100
Deflect angle (rad)	0.211e-2	0.571e-2	-0.113e-2
The angle of rotation (rad)	0.014	0.014	0.015
Straightening stroke (mm)	6.797	6.726	7.424
Straightening moment (Mpa)	5.702e5	5.695e5	5.686e5
Final straightness (mm)		2.374	

in Fig. 16, 4-step FSMSP can correct the straightness error to 1.226mm, which was more effective than 3-step and 5-step FSMSP. In terms of VSMSP, a 4-step process can improve the straightness error of 'S'-shape deflection curve to 0.181mm in this case.

C. MULTI-PEAK DEFLECTION CURVE

Considering the complexity of the multi-peak deflection curve, the search of span size needs to ensure that the deflection curve is a single arc in every straightening step, and thus the number of straightening steps is normally more than that in the other cases, resulting in an increase of the control points.

A curve simulating the deflection curve was created by using the sine function $f(x) = 3\sin(2\pi x/L_W)$ over [0,1000], the span sizes were 340mm, 340mm and 320mm for

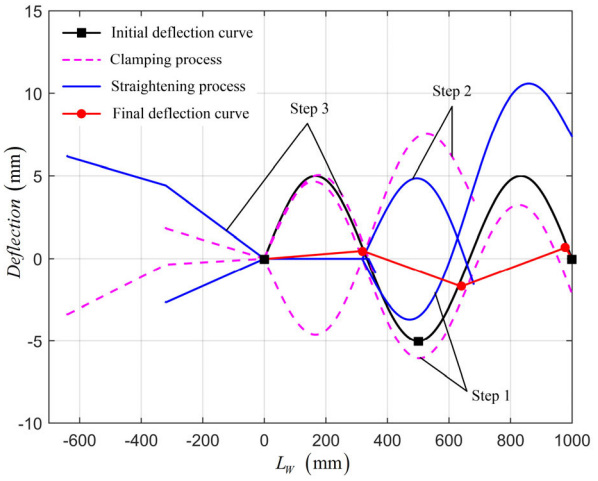

FIGURE 19. Theoretical results of the major straightening stage for the multi-peak deflection curve.

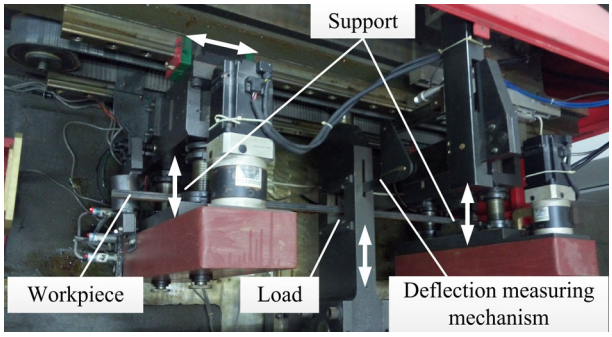

(a) Straightening experiments

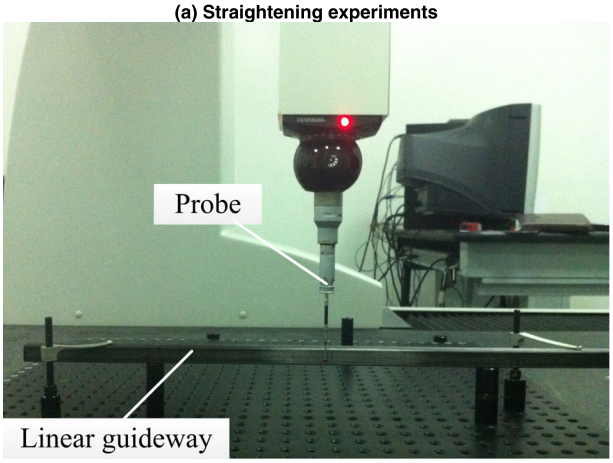

(b) Measurement of deflection curve

FIGURE 20. Experimental set-up used in the VSMSP of the sample linear guideway.

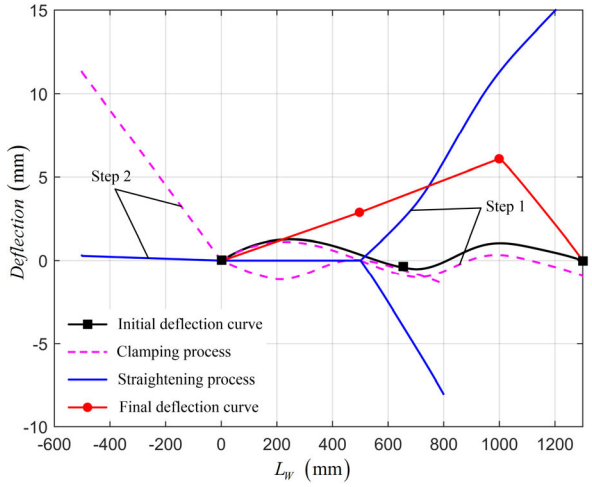

(a) Major straightening stage

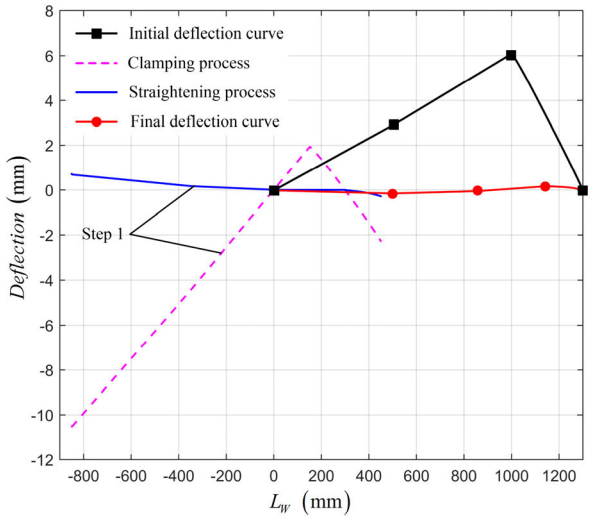

(b) Fine straightening stage

FIGURE 21. Theoretical results for the VSMSP of the sample linear guideway.

the 3-step straightening process, considering the extremum of the deflection curve, as listed in Table 5. It can be detected that the straightness of the deflection curve was significantly improved from 6mm to 0.577mm in theory as shown in Fig. 17. In this case, it was not necessary to perform the fine straightening stage. A 3-step FSMSP of the deflection curve in this case can correct the straightness error to 2.431mm as shown in Fig.18, while the 4-step and 5-step FSMSP had worse performances.

If the span sizes are unable to adapt to the profile of the deflection curve very well, the deflection curve would be a polyline with large angles on it caused by the rotation of the workpiece during the different straightening steps, thereby slightly improving the straightness. In some extreme cases, the fine straightening stage would not be useful to improve the straightness of the deflection curve.

In terms of the deflection curve $f(x) = 5\sin(3\pi x/L_W)$ over [0,1000], the major straightening stage was divided

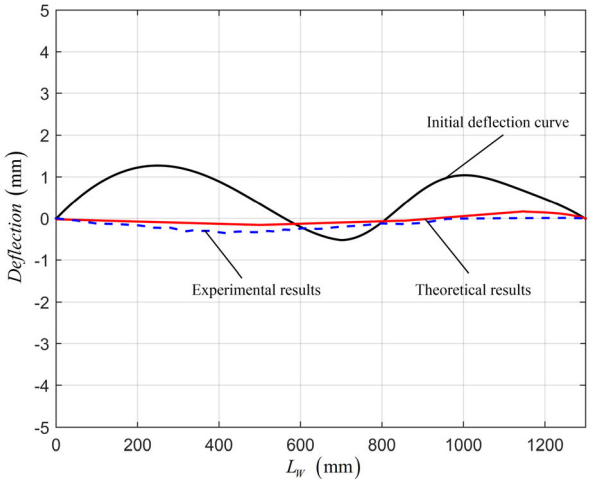

FIGURE 22. Comparison of theoretical and experimental results after the VSMSP of the sample linear guideway.

into 3 steps as listed in Table 6. It can be noticed that the deflection curve with straightness error 10mm was improved by 76.26% to 2.374mm after the major straightening stage as shown in Fig. 19. However, the fine straightening stage cannot improve the straightness error any more in this case.

V. VERIFICATIONS

The proposed multistep straightening strategy was verified using LG-series linear guideways on the straightening machine ROSE-JZ0 (see Fig. 20(a)). Before and after the VSMSP, the deflection curve of the sample linear guideway was measured by using a three-coordinate measuring instrument (Brown & Sharpe: GLOBAL Performance 1287) with the accuracy of 1 μm (see Fig. 20(b)). The experimental results were also compared to the theoretical results.

Using the proposed multistep straightening strategy for the VSMSP, the theoretical results were demonstrated in Fig. 21, and the straightening parameters were listed in Table 7. The VSMSP of the sample linear guideway was divided into 3 straightening steps, consisting of two straightening steps in the major straightening stage and one straightening step in the fine straightening stage. The length of the remaining part was detected as 300mm, which had already met the requirements of the straightness. The one-step fine straightening was performed on the third control point. The deflection curves, in both theory and experiment, were compared as shown in Fig. 22, demonstrating that the straightness of the sample linear guideway was improved by 81.87% and 80.04%, respectively. The initial straightness error of the sample linear guideway was 1.793mm, while the straightness errors were 0.325mm and 0.358mm, in theory and experiment, respectively. There was a good agreement between the theoretical and experimental results, despite the errors caused by the errors of the measurement system and the simplifications of straightening model.

TABLE 7. Parameters for the VSMSP of the sample linear guideway.

No.	1	2	3
Span size (mm)	500	500	300
Initial deflection (mm)	1.103	1.202	1.987
Standard deflection (mm)	2.300	2.300	5.600
The angle of rotation (rad)	0.022	0.021	0.013
Straightening stroke (mm)	5.5491	5.675	3.783
Straightening moment (Mpa)	4.868e5	4.897e5	5.461e5
Final straightness (mm)		0.325	

VI. CONCLUSION

In this paper, the variable span multistep straightening strategy is proposed to improve straightening accuracy and reduce the number of straightening steps for the multistep straightening of long linear guideways with complex shapes. Straightening facilities can determine the nominal straightening moment and stroke, the maximum span size and the measurement range for the deflection. These factors as well as unexpected deformation are considered in the span-size searching algorithm, which is the core step in the mathematical model of the VSMSP. Based on the proposed straightening approach, a theoretical analysis has been performed on the typical types of deflection curves, including single-arc shape, 'S' shape and multi-peak shape. The straightening experiments are performed on the ROSE-JZ50 straightening machine and the results demonstrate that this approach can help improve the straightness significantly.

However, the accuracy and efficiency of VSMSP is restricted by the comprehensive factors including the capability of straightening facilities, the shape of deflection curves and the planning of straightening steps. The future work needs to establish an assessment model balancing the straightening accuracy and efficiency. Besides, the intelligent algorithms would be employed to optimize the VSMSP.

ACKNOWLEDGMENT

(Yongquan Zhang and Hong Lu contributed equally to this work.)

REFERENCES

[1] M. Rahmani and F. Bleicher, "Experimental and numerical studies of the influence of geometric deviations in the performance of machine tools linear guides," *Procedia CIRP*, vol. 41, pp. 818–823, Jan. 2016.
[2] G. He, C. Huang, L. Guo, G. Sun, and D. Zhang, "Identification and adjustment of guide rail geometric errors based on BP neural network," *Meas. Sci. Rev.*, vol. 17, no. 3, pp. 135–144, 2017.
[3] C. B. Biempica, J. J. del Coz Daíz, P. J. G. Nieto, and I. P. Sánchez, "Nonlinear analysis of residual stresses in a rail manufacturing process by FEM," *Appl. Math. Model.*, vol. 33, no. 1, pp. 34–53, 2009.
[4] A. Pernía, F. J. Martínez-de-Pisón, J. Ordieres, F. Alba, and J. Blanco, "Fine tuning straightening process using genetic algorithms and finite element methods," *Ironmaking Steelmaking*, vol. 37, no. 2, pp. 119–125, 2010.
[5] R. C. Spoorenberg, H. H. Snijder, and J. C. D. Hoenderkamp, "Finite element simulations of residual stresses in roller bent wide flange sections," *J. Construct. Steel Res.*, vol. 67, no. 1, pp. 39–50, 2011.
[6] R. Kaiser, M. Stefenelli, T. Hatzenbichler, T. Antretter, M. Hofmann, J. Keckes, and B. Buchmayr, "Experimental characterization and modelling of triaxial residual stresses in straightened railway rails," *J. Strain Anal. Eng. Des.*, vol. 50, no. 3, pp. 190–198, 2014.
[7] P.-A. Eggertsen and K. Mattiasson, "On the modelling of the bending–unbending behaviour for accurate springback predictions," *Int. J. Mech. Sci.*, vol. 51, no. 7, pp. 547–563, 2009.
[8] A. N. Gergess and R. Sen, "Cambering structural steel I-girders using cold bending," *J. Construct. Steel Res.*, vol. 64, no. 12, pp. 407–417, 2008.
[9] F. Kosel, T. Videnic, T. Kosel, and M. Brojan, "Elasto-plastic springback of beams subjected to repeated bending/unbending histories," *J. Mater. Eng. Perform.*, vol. 20, no. 6, pp. 846–854, 2011.
[10] S.-L. Zang, M.-G. Lee, L. Sun, and J. H. Kim, "Measurement of the Bauschinger behavior of sheet metals by three-point bending springback test with pre-strained strips," *Int. J. Plasticity*, vol. 59, pp. 84–107, Aug. 2014.
[11] L. Ma, Z. Ma, W. Jia, Y. Lv, Y. Jiang, H. Xu, and P. Liu, "Research and verification on neutral layer offset of bar in two-roll straightening process," *Int. J. Adv. Manuf. Technol.*, vol. 79, nos. 9–12, pp. 1519–1529, 2016.
[12] P. Hou, H. Zhao, Z. Ma, S. Zhang, J. Li, X. Dong, Y. Sun, and Z. Zhu, "Influence of punch radius on elastic modulus of three-point bending tests," *Adv. Mech. Eng.*, vol. 8, no. 5, pp. 1–8, 2016.
[13] F. Mujika, A. Arrese, I. Adarraga, and U. Oses, "New correction terms concerning three-point and four-point bending tests," *Poly Test.*, vol. 55, pp. 25–37, Oct. 2016.
[14] M. A. Sofuoğlu, S. Gürgen, F. H. Çakır, and S. Orak, "Springback behavior of AA6082T6 tubes in three-point bending operation," *Procedia Eng.*, vol. 182, pp. 658–664, Jan. 2017.
[15] Y. Zhang, H. Lu, H. Ling, Y. Lian, and M. Ma, "Analytical model of a multi-step straightening process for linear guideways considering neutral axis deviation," *Symmetry-Basel*, vol. 10, no. 8, p. 316, 2018.
[16] Y. Song, "Load-deflection model for T-section rail Press straightening process under lateral loads," *Cluster Comput.*, to be published. doi: 10.1007/s10586-018-1710-5.
[17] J. Zhao and X. Song, "Control strategy of multi-point bending one-off straightening process for LSAW pipes," *Int. J. Adv. Manuf. Technol.*, vol. 72, nos. 9–12, pp. 1615–1624, 2014.
[18] S. C. Kim and S. C. Chung, "Synthesis of the multi-step straightness control system for shaft straightening processes," *Mechatronics*, vol. 12, no. 1, pp. 139–156, 2002.
[19] K. Wang, B. Wang, and C. Yang, "Research on the multi-step straightening for the elevator guide rail," *Procedia Eng.*, vol. 16, pp. 459–466, Jan. 2011.
[20] Y. Zhang, H. Lu, X. Zhang, H. Ling, W. Fan, Q. Wei, and Y. Lian, "A novel control strategy for the multi-step straightening process of long/extra-long linear guideways," *Proc. Inst. Mech. Eng. C, J. Mech. Eng. Sci.*, vol. 233, no. 9, pp. 2959–2975, 2019. doi: 10.1177/0954406218800117.
[21] *An ASME National Standard-Engineering Drawing and Related Documentation Practices: Dimensioning and Tolerancing*, ASME Standard Y14.5M, 1994.

YONGQUAN ZHANG was born in 1989. He received the B.S. degree in mechanical engineering from the Wuhan University of Technology, China, in 2011, where he is currently pursuing the Ph.D. degree in mechanical engineering. He is also a Visiting Research Ph.D. Student in remanufacturing with the University of Birmingham. His current research interests include plastic mechanics and control technology.

HONG LU received the B.S. and M.S. degrees in mechanical manufacturing from the Huazhong University of Science and Technology, in 1987 and 1990, respectively, and the Ph.D. degree in mechanical engineering from the Wuhan University of Technology, Wuhan, China, in 2000. She is currently a Full Professor with the School of Mechanical and Electronic Engineering, Wuhan University of Technology, China. She has authored three books, more than 60 articles, and more than 20 inventions. Her research interests include mechanical CAD/CAM, synchronous control technology, and mechatronics.

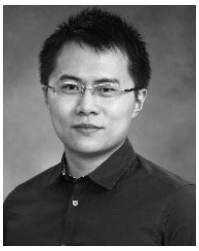

YONGJING WANG received the B.Eng. degree (Hons.) in electronic and electrical engineering and the Ph.D. degree in engineering from the University of Birmingham, U.K., in 2013 and 2016, respectively, and the B.Eng. degree in automatic control from the Harbin Institute of Technology, China. He is currently a Research Fellow with the Department of Mechanical Engineering, School of Engineering, University of Birmingham, where he is also a member with the Autonomous Remanufacturing Laboratory. His current research interests include the automation of complex and flexible industrial processes.

XINBAO ZHANG received the B.S. and M.S. degrees and the Ph.D. degree in instrument science and technology from the Huazhong University of Science and Technology, Wuhan, China, in 2002, where he is currently a Professor with the School of Mechanical Science and Engineering. He has authored more than 30 articles, and more than 5 inventions. His research interests include mechanical design and manufacturing, measurement technology and instruments, and tolerance theory.

JINGLIN ZHANG was born in 1993. He received the B.S. degree in mechanical engineering and automation from the Hubei University of Automotive Technology, China, in 2016, and the M.S. degree in mechanical engineering from the Wuhan University of Technology, China, in 2019. His current research interest includes metal straightening.

HE LING received the B.S. degree in mechanical engineering and automation from Huazhong Agricultural University, Wuhan, China, in 2004, and the M.S. and Ph.D. degrees in mechanical engineering from the Wuhan University of Technology, Wuhan, China, in 2007 and 2011, respectively, where he has been an Associate Professor, since 2012. His research interest includes the intelligent manufacturing technology and equipment.